Natural Convection from a Plane Vertical Porous Surface in Non-Isothermal Surroundings

S.C. Saha[1], C. Akhter[1], M.A. Hossain[2]

[1]School of Computer Science, IBAIS University, Dhaka, Bangladesh
s_c_saha@yahoo.com

[2]Dept. of Mathematics, Dhaka University, Dhaka, Bangladesh

Abstract. In this paper, laminar natural convection flow from a permeable and isothermal vertical surface placed in non-isothermal surroundings is considered. Introducing appropriate transformations into the boundary layer equations governing the flow derives non-similar boundary layer equations. Results of both the analytical and numerical solutions are then presented in the form of skin-friction and Nusselt number. Numerical solutions of the transformed non-similar boundary layer equations are obtained by three distinct solution methods, (i) the perturbation solutions for small ξ (ii) the asymptotic solution for large ξ (iii) the implicit finite difference method for all ξ where ξ is the transpiration parameter. Perturbation solutions for small and large values of ξ are compared with the finite difference solutions for different values of pertinent parameters, namely, the Prandtl number Pr, and the ambient temperature gradient n.

Keywords: porous surface, non-isothermal surroundings, body force

1 Introduction

Thermal boundary layer non-similarity may result from various cases. Perhaps the most common cause is the non-similarity of the velocity boundary layer. In turn, there are various factors, which may give rise to velocity boundary layer non-similarity, among which are: (i) stream wise variations in the free stream velocity, (ii) surface mass transfer (iii) transverse curvature and (iv) non-isothermal surroundings. Also thermal boundary layer can be non-similar

even when the velocity boundary layer is similar, as will occur when stream wise variations in the surface temperature, surface heat flux or volume heat generations are not restricted to certain simple forms. Thus, there are many classes of non-similarity in thermal boundary layer. The different classes of thermal boundary layer non-similarity are generated by mathematical systems, which differ in various details one from other. Sparrow and Yu [1] used the local non-similarity method to solve the thermal boundary layer equation for the steady flow with uniform free stream velocity in the presence of surface mass-flux, transverse curvature, stream wise variations of the free stream velocity, and stream wise variations of the surface temperature. Kao [2] applied the shooting method technique as described by Nachtsheim and Swigert [3] to solve the non-similarity boundary layer and thermal boundary layer equations for the forced convection along a flat plate with arbitrary suction or injection at the wall.

Many free convection processes occur in environments with temperature stratification. A room that is heated by electrical wires embedded in the ceiling may be thermally stratified. A room fire with an open door or window through which fresh air is supplied near the bottom is another example of a thermally stratified situation. Several attempts have been made in recent years to investigate the problem of natural convection over a vertical wall in a stratified medium due to its obvious importance. Early studies were focused on seeking similarity solution because the similar variables can give great physical insight with minimal efforts. Yang [4] first presented a general approach for obtaining similarity solutions to a class of problems for a non-isothermal vertical wall surrounded by an isothermal atmosphere. For laminar free convection along a vertical plate, Cheesewright [5] obtained similarity solutions dealing with various types of non-uniform ambient temperature distributions by using the technique of Yang [4]. None of the variety of cases presented by Cheesewright [5] and Yang et al [6] included a case in which the wall was isothermal and the ambient atmosphere had a linearly increasing temperature distribution. Fujii *et al.* [7] presented both analytical and experimental results for a temperature stratification in which the ambient temperature distribution varies with x. Piau [8] carried out a study in which both the plate temperature and the ambient

temperature varied with power of x. Later, Eichhorn *et al.* [9] presented experimental heat transfer results for isothermal spheres and horizontal cylinders.

Chen and Eichhorn [10] concluded that a similarity solution of the problem of an isothermal heated wall in a linearly stratified stable atmosphere was not possible and hence used the local non-similarity approach to solve the problem. Non-similarity solutions dealing with various types of non-uniform ambient temperature had also been Venkatachala and Nath [11] in which the local variable introduced depending on the stratification of the media had also produced temperature.

Very recently, Chamkha and Khaled [12], investigated the problem of steady, hydro magnetic simultaneous heat and mass transfer by mixed convection flow over a vertical plate embedded in a uniform porous medium with a stratified free stream and taking into account the presence of thermal dispersion is investigated for the case of power-law variations of both the wall temperature and concentration by using local-similarity form.

A problem of interest and importance in some applications concerns the effect of blowing and suction in a natural convection boundary layer. This situation would arise, for instance, if heat transfer from a porous surface were being investigated and fluid were being added to or removed from the flow. For the flat plate with suction Emmons and Leigh [13] found solutions of the momentum equation, while the corresponding heat transfer results for the isothermal porous plate were presented by Schilichting and Bussemann [14] and Hartnett and Eckert [15]. These later investigations also included heat transfer and skin-friction result for an isothermal plane-stagnation region with wall suction. A problem of greater practical applicability is that of a uniform blowing or suction velocity v_0. But this does not give similarity. Sparrow and Cess [16] considered this case for an isothermal surface. They employed a perturbation technique. Merkin [17] obtained asymptotic expansion, as $x \to \infty$, for temperature and velocity. Clarke [18] obtained the next approximation to the solution of the Navier-Stocks equations for large Grashof number and considered density variations, avoiding the Boussinesq approximation. Aroesty and Cole [19] also considered strong blowing for bodies of general shape.

In this paper, we have considered a permeable vertical surface, which is immersed, in a thermally stratified medium. Here the ambient temperature is assumed to be power function of x. Using appropriate transformations the boundary layer equations for momentum and heat transfer are reduced to non-similar partial equations which arises due to the transpiration parameter ξ. Solutions of these equations are obtained, for all values of ξ, which employing the finite difference method together with the Keller-box elimination technique. Appropriate perturbation solutions are also obtained for small and large values of ξ which then compared with the finite difference solutions for different values of pertinent parameters, such as, the Prandtl number and the ambient temperature gradient. Results are presented graphically in terms of local skin-friction as well as the local Nusselt number.

2 Mathematical formulation

Let us consider the steady two-dimensional viscous incompressible fluid on a vertical porous surface immersed in non-isothermal surroundings. Let x denotes distance along the surface from the leading edge and y is the normal distance from the surface. The wall temperature is considered as uniform at θ_w and the ambient temperature $\theta_\infty(x)$ is assumed to vary as x^n.

The flow configuration and the co-ordinate system are shown in Fig. 1. With respect to the co-ordinate system, the equations of continuity, momentum
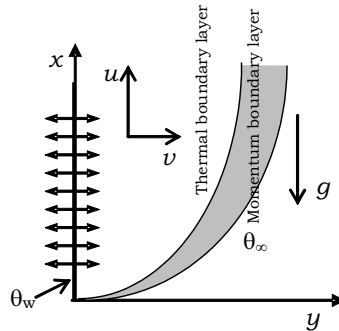

Fig. 1. The flow configuration and co-ordinate system.

and energy, which govern the flow and heat transfer in a laminar boundary

layer in the presence of a body force are respectively,

$$\frac{\partial u}{\partial x} + \frac{\partial v}{\partial y} = 0, \tag{1}$$

$$u\frac{\partial u}{\partial x} + v\frac{\partial u}{\partial y} = -\frac{1}{\rho}\frac{dp}{dx} + \Omega + \nu\frac{\partial^2 u}{\partial y^2}, \tag{2}$$

$$u\frac{\partial \theta}{\partial x} + v\frac{\partial \theta}{\partial y} = \frac{\kappa}{\rho c_p}\frac{\partial^2 \theta}{\partial y^2} \tag{3}$$

where u and v are the fluid velocity components along x- and y-axis which are parallel and normal to the plate respectively, Ω is the body force term in boundary layer equation, ν is the kinematic viscosity, θ is the temperature, p is the pressure, ρ is the density, κ is the thermal conductivity, C_p is the specific heat capacity.

If consideration is restricted to a region of plate, having a temperature everywhere greater than or equal to that of its surroundings, we can write $\Omega = -g$. It should be noted that for cases in which $\theta_w - \theta_\infty$ decreases with distance up the plate, the above restrictions lead to the consideration of a region of limited extent rather than the semi-infinite region usually considered in boundary-layer problems.

Outside the boundary layer equation (2),

$$u_\infty\frac{\partial u_\infty}{\partial x} + \frac{1}{\rho_\infty}\frac{dp}{dx} + g = 0 \tag{4}$$

where u_∞ the free stream velocity. Since we can consider pure free convection flow, $u_\infty = 0$. From (2) and (4),

$$\rho\left(\frac{\partial u}{\partial t} + u\frac{\partial u}{\partial x} + v\frac{\partial u}{\partial y}\right) = -g(\rho - \rho_\infty) + \mu\frac{\partial^2 u}{\partial y^2}. \tag{5}$$

Following Ostrach [20], property variations are assumed to be important only in so far as they affect the body force term, and the density variation is represented by,

$$\rho = \rho_0\big[1 - \beta(\theta - \theta_0)\big]$$

where ρ_0 is the density at an arbitrary reference temperature θ_0, β is the coefficient of cubical expansion ($1/T_0$ for a perfect gas). Now equation (5)

becomes

$$u\frac{\partial u}{\partial x} + v\frac{\partial u}{\partial y} = g\beta(\theta - \theta_0) + \nu\frac{\partial^2 u}{\partial y^2}. \tag{6}$$

Now the equations are,

$$u\frac{\partial u}{\partial x} + v\frac{\partial u}{\partial y} = 0, \tag{7}$$

$$u\frac{\partial u}{\partial x} + v\frac{\partial u}{\partial y} = g\beta(\theta - \theta_\infty) + \nu\frac{\partial^2 u}{\partial y^2}, \tag{8}$$

$$u\frac{\partial \theta}{\partial x} + v\frac{\partial \theta}{\partial y} = \frac{\kappa}{\rho c_p}\frac{\partial^2 \theta}{\partial y^2}. \tag{9}$$

The corresponding boundary conditions

$$\begin{aligned}
u = 0, \quad v = -v_0, \quad \theta = \theta_w \quad \text{at} \quad y = 0, \\
u = 0, \quad \theta = \theta_\infty(x) \quad \text{as} \quad y \to \infty.
\end{aligned} \tag{10}$$

For suction v_0 is positive and for injection it is negative.

It may be noted that equation (8) is identical with the corresponding equation for the case $\theta_\infty = const$. The above derivation has been given because it is not felt that this identity is obvious.

The continuity equation (7) is automatically satisfied when a stream function ψ is introduced, i.e.

$$u = \frac{\partial \psi}{\partial y}, \quad v = -\frac{\partial \psi}{\partial x}.$$

Now the equation (8) and (9) become,

$$\frac{\partial \psi}{\partial y}\frac{\partial^2 \psi}{\partial x \partial y} - \frac{\partial \psi}{\partial x}\frac{\partial^2 \psi}{\partial y^2} = g\beta(\theta - \theta_\infty) + \nu\frac{\partial^3 \psi}{\partial y^3}, \tag{11}$$

$$\frac{\partial \psi}{\partial y}\frac{\partial \theta}{\partial x} - \frac{\partial \psi}{\partial x}\frac{\partial \theta}{\partial y} = \frac{\kappa}{\rho c_p}\frac{\partial^2 \theta}{\partial y^2}. \tag{12}$$

It is convenient to make these equations dimensionless by writing

$$\begin{aligned}
X = \frac{x}{L}, \quad Y = \frac{y}{L}, \quad \Psi = \frac{\psi}{\nu}, \\
G = \frac{g\beta L^3(\theta - \theta_0)}{\nu^2}, \quad G_\infty = \frac{g\beta L^3(\theta_\infty - \theta_0)}{\nu^2}
\end{aligned} \tag{13}$$

where L is characteristic length. Now equation (11) and (12) become,

$$\frac{\partial \Psi}{\partial Y} \frac{\partial^2 \Psi}{\partial X \partial Y} - \frac{\partial \Psi}{\partial X} \frac{\partial^2 \Psi}{\partial Y^2} = G - G_\theta + \frac{\partial^3 \Psi}{\partial Y^3}, \tag{14}$$

$$\frac{\partial \Psi}{\partial Y} \frac{\partial G}{\partial X} - \frac{\partial \Psi}{\partial X} \frac{\partial G}{\partial Y} = \frac{1}{Pr} \frac{\partial^2 G}{\partial Y^2} \tag{15}$$

with the boundary conditions,

$$\Psi_Y = 0, \quad \Psi_X = s, \quad G = G_w \quad \text{at} \quad Y = 0,$$
$$\Psi_Y = 0, \quad G = G_\infty(x) \quad \text{as} \quad Y \to \infty. \tag{16}$$

3   Transformation of the equations

We may introduce the new transformation:

$$\Psi = X^{\frac{n+3}{4}} \big[f(\eta, \xi) \pm \xi \big], \ \Phi(\eta, \xi) = \frac{G - G_\infty}{G_w - G_\infty}, \ \eta = Y X^{\frac{n-1}{4}}$$
$$G_w - G_\infty = X^n, \ \xi = X^{\frac{1-n}{4}} s, \ s = \frac{VL}{\nu}, \ G_w = \frac{g \beta L^3 (\theta_w - \theta_\infty)}{\nu^2}. \tag{17}$$

Thus the momentum and energy equations are,

$$f''' + \frac{n+3}{4} f f'' - \frac{n+1}{2} f'^2 + \Phi \pm \xi f''$$
$$= \frac{1-n}{4} \xi \left(f' \frac{\partial f'}{\partial \xi} - f'' \frac{\partial f}{\partial \xi} \right), \tag{18}$$

$$\frac{1}{Pr} \Phi'' + \frac{n+3}{4} f \Phi' - n f'(\Phi - 1) \pm \xi \Phi'$$
$$= \frac{1-n}{4} \xi \left(f' \frac{\partial \Phi}{\partial \xi} - \Phi' \frac{\partial f}{\partial \xi} \right) \tag{19}$$

with the boundary conditions,

$$f = f' = 0, \quad \Phi = 1 \quad \text{at} \quad \eta = 0,$$
$$f' = 0, \quad \Phi = 0 \quad \text{as} \quad \eta \to \infty. \tag{20}$$

From solving equations (18) and (19), we find the value of $f''(0)$ and $\theta'(0)$. Now dividing $f''(0)$ by $\sqrt{2}$ and multiplying $\theta''(0)$ by $\sqrt{2}$ and compare these results with the Cheesewright [5] result in Table 1.

Table 1. Numerical values of $f''(0)$ and $\theta''(0)$ taking $Pr = 0.708$ and $\xi = 0.0$

	$f''(0)$		$\theta'(0)$	
n	Cheesewright [5]	Present	Cheesewright [5]	Present
-0.15	0.65949	0.65817	-0.55423	-0.55371
-0.30	0.64099	0.64097	-0.50414	-0.60413

Here we are proposing to find solutions of the equations (18) and (19) along with the boundary conditions (20) employing the three different solution methods, namely (i) the series solution for small ξ,(ii) the asymptotic solution for large ξ and (iii) the implicit finite difference method together with Keller-box method for all ξ.

4 Physical quantity

The important physical quantities are wall shearing stress factor, τ_w, and the heat transfer rate $q(x)$.

The magnitude of τ_w and $q(x)$ may be defined as,

$$\tau_w = \mu\left(\frac{\partial u}{\partial y}\right)_{y=0}, \quad q(x) = -\kappa\left(\frac{\partial \theta}{\partial y}\right)_{y=0}. \tag{21}$$

The dimensionless shearing stress factor or the skin-friction, C_f, may be expressed as follows:

$$C_f = \frac{2\tau_w}{\rho\left(\frac{\nu}{x}\right)^2}. \tag{22}$$

Using the quantity of equation (21) and the transformation (17) in equation (22), we investigate the local skin-friction in terms of the dimensionless shearing stress, C_f, given as

$$\frac{C_f}{Gr_x^{3/4}} = f''(0, \xi). \tag{23}$$

We may define a non-dimensional coefficient of heat transfer in terms of nusselt number Nu_x which is known as,

$$Nu_x = \frac{q(x)x}{\kappa\Delta\theta_0}. \tag{24}$$

Substituting the transformation (17) and (21) in (24), we obtain the rate of heat transfer, in terms of the dimensionless Nusselt number, given as,

$$\frac{Nu_x}{Gr_x^{1/4}} = -\Phi'(0, \xi).$$

(25)

5 Solution methodologies

We are proposing here to find solutions of the equations (18) and (19) along with the boundary conditions (20) employing the three different solution methods: namely (a) the series solution for small ξ (b) the asymptotic solution for large ξ and (c) the implicit finite difference method together with Keller-box method for all ξ.

5.1 Perturbation solution for small ξ (PS)

We assume the following expansions for the functions f and Φ for small ξ

$$f(\eta, \xi) = \sum_{i=0}^{n} (\pm \xi)^i f_i(\eta), \quad \Phi(\eta, \xi) = \sum_{i=0}^{n} (\pm \xi)^i \Phi_i(\eta).$$

(26)

Substituting the expression (26) into the equations (18)–(20) and equating the coefficient of various powers of ξ, the following sets of equations can be obtained:

$$f_0''' + \frac{n+3}{4} f_0 f_0'' - \frac{n+1}{2} f_0'^2 + \Phi_0 = 0,$$

(27)

$$\frac{1}{Pr} \Phi_0'' + \frac{n+3}{4} f_0 \Phi_0' - n f_0'(\Phi_0 - 1) = 0$$

(28)

boundary conditions are,

$$f_0 = f_0' = 0, \quad \Phi_0 = 1 \quad \text{at} \quad \eta = 0,$$
$$f_0' = 0, \quad \Phi_0 = 0 \quad \text{as} \quad \eta \to \infty.$$

(29)

The higher order equations, for $i \geq 1$,

$$f_i''' + f_{i-1}'' + \frac{1}{4} \sum_{r=0}^{i} \left[(n+3) + (1-n)r \right] f_r f_{i-r}''$$
$$- \frac{1}{2} \sum_{r=0}^{i} \left[(n+1) + \frac{1-n}{2} r \right] f_r' f_{i-r}' + \Phi_i = 0,$$

(30)

$$\frac{1}{Pr}\Phi_i'' + \Phi_{i-1}' + \frac{1}{4}\sum_{r=0}^{i}\left[(n+3) + (1-n)r\right]f_r\Phi_{i-r}'$$
$$-\sum_{r=0}^{i}\left[n + \frac{1-n}{4}r\right]f_{i-r}'\Phi_r + nf_i' = 0 \tag{31}$$

boundary conditions are,

$$f_i = f_i' = 0, \quad \Phi_i = 1 \quad \text{at} \quad \eta = 0,$$
$$f_i' = 0, \quad \Phi_i = 0 \quad \text{as} \quad \eta \to \infty. \tag{32}$$

We know the solutions for the functions f_i and θ_i ($i = 0, 1, 2$) and their derivatives from the above sets of equations, we obtain the values of the local skin friction.

$$\frac{C_f}{Gr_x^{3/4}} = f''(0, \xi) = \sum_{i=0}^{n}\xi^i f_i^n(0). \tag{33}$$

The Nusselt number is defined as,

$$\frac{Nu_x}{Gr_x^{1/4}} = -\theta'(0, \xi) = \sum_{i=0}^{n}\xi^i\theta_i'(0). \tag{34}$$

For example, taking Prandtl number $Pr = 0.708$ and $n = 0.3$, the above series (33) and (34) can be written as

$$\frac{C_f}{Gr_x^{3/4}} = 0.99290 + 0.19379\xi - 0.11206\xi^2,$$
$$\frac{Nu_x}{Gr_x^{1/4}} = 0.28559 + 0.31559\xi + 0.11505\xi^2.$$

Substituting the particular value of the suction parameter ξ (i.e. $\xi = 0.1$) in the above expression, we obtain the numerical values of the skin-friction and heat transfer are 1.0111584 and 03182995 respectively. Similarly, for the different values of suction parameter ξ and the ambient temperature gradient n we can find the values of $C_f/Gr_x^{3/4}$ and $Nu/Gr_x^{3/4}$ by using above expression. The result of these for different values of Prandtl number, have been compared that of the other methods in Table 2 and for different values of ambient temperature gradient n, have been compared the other methods in Fig. 2.

Table 2. Numerical values of the (a) skin-friction and (b) heat-transfer obtained by different methods for different values of ξ while $Pr = 0.1$ and $Pr = 0.708$ at $n = 0.3$

(a) Skin-friction

| ξ | $C_f/Gr_x^{3/4} = f''(0, \xi)$ | | | |
| | $Pr = 0.1$ | | $Pr = 0.708$ | |
	PS & AS	FD	PS & AS	FD
-1.0	$0.72449p$	0.75159	$0.68035p$	0.73300
-0.6	$0.90024p$	0.90928	$0.83240p$	0.85065
-0.2	$1.08294p$	1.09077	$0.94402p$	0.95891
0.0	$1.17690p$	1.18382	$0.98467p$	0.99612
0.6	$1.46921p$	1.48230	$1.04596p$	1.04522
1.0	$1.67278p$	1.67284	$1.03627p$	1.01265
2.0		2.04193		0.68269
4.0		2.11506		0.34165
5.0	$1.92312a$	1.88208	$0.28257a$	0.27344
20.0	$0.49992a$	0.50266	$0.07062a$	0.07418
60.0	$0.16667a$	0.16665	$0.02354a$	0.04967
100	$0.10000a$	0.09576	$0.01412a$	0.03673

(b) Heat-transfer

| ξ | $C_f/Gr_x^{3/4} = f''(0, \xi)$ | | | |
| | $Pr = 0.1$ | | $Pr = 0.708$ | |
	PS & AS	FD	PS & AS	FD
-1.0	$0.09482p$	0.09089	$0.08754p$	0.07047
-0.6	$0.11274p$	0.10836	$0.13965p$	0.12961
-0.2	$0.13185p$	0.12770	$0.23018p$	0.22122
0.0	$0.14185p$	0.13846	$0.28982p$	0.28391
0.6	$0.17364p$	0.17192	$0.52624p$	0.53625
1.0	$0.19633p$	0.19488	$0.73178p$	0.74797
2.0		0.25759		1.42883
4.0		0.41250		2.85938
5.0	$0.50218a$	0.50524	$3.54141a$	3.56709
20.0	$2.00003a$	2.00349	$14.1600a$	14.2685
60.0	$6.00000a$	5.99973	$42.4800a$	43.6236
100	$10.0000a$	9.99501	$70.8000a$	70.8295

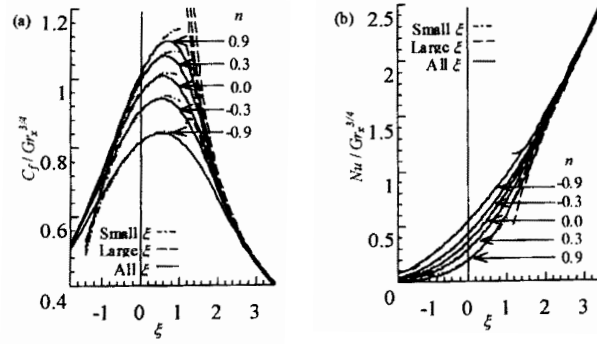*Here p stands for perturbation solution and a stands for asymptotic solution.

Fig. 2. (a) Dimensionless skin-friction and (b) dimensionless heat-transfer for different values of ξ as well as n with the selected Prandtl number $Pr = 0.708$.

5.2 Asymptotic solution for large ξ (AS)

Now, attention has been given to the behavior of the solution of the equations (18) and (19) when ξ is positively large. The following substitutions for the asymptotic solution are introduced:

$$f(\eta, \xi) = \xi^{-3}\widehat{f}(\widehat{\eta}, \xi), \quad \Phi(\eta, \xi) = \widehat{\Phi}(\widehat{\eta}, \xi), \quad \widehat{\eta} = \xi\eta. \tag{35}$$

Substituting the transformation (35) to the equation (18)–(20) we get the following equations,

$$\widehat{f}''' + \widehat{f}'' + n\xi^{-4}(\widehat{f}\widehat{f}'' - \widehat{f}'^2) + \widehat{\Phi}$$
$$= \frac{1-n}{4}\xi^{-3}\left(\widehat{f}'\frac{\partial \widehat{f}'}{\partial \xi} - \widehat{f}''\frac{\partial \widehat{f}}{\partial \xi}\right), \tag{36}$$

$$\frac{1}{Pr}\widehat{\Phi}'' + \widehat{\Phi}' + n\xi^{-4}\left(\widehat{f}\widehat{\Phi}' - \widehat{f}'(\widehat{\Phi} - 1)\right)$$
$$= \frac{1-n}{4}\xi^{-3}\left(\widehat{f}'\frac{\partial \widehat{\Phi}}{\partial \xi} - \widehat{\Phi}'\frac{\partial \widehat{f}}{\partial \xi}\right) \tag{37}$$

with the boundary conditions,

$$\widehat{f} = \widehat{f}' = 0, \quad \widehat{\Phi} = 1 \quad \text{at} \quad \widehat{\eta} = 0,$$
$$\widehat{f}' = 0, \quad \widehat{\Phi} = 0 \quad \text{as} \quad \widehat{\eta} \to \infty. \tag{38}$$

162

We assume the following expansions for the functions $\widehat{f}$ and $\widehat{\Phi}$ are of the form for large ξ.

$$\widehat{f}(\widehat{\eta}, \xi) = \sum_{i=0}^{n} \xi^{-4i} \widehat{f}_i(\widehat{\eta}), \quad \widehat{\Phi}(\widehat{\eta}, \xi) = \sum_{i=0}^{n} \xi^{-4i} \widehat{\Phi}_i(\widehat{\eta}). \tag{39}$$

Substituting the expression (39) into the equations (36)–(38) and equating the coefficients up to the (ξ^{-4}), we obtain the followings equations:

For $\xi^0 = 1$,

$$\widehat{f}_0''' + \widehat{f}_0'' + \widehat{\Phi}_0 = 0, \tag{40}$$

$$\frac{1}{Pr} \widehat{\Phi}_0'' + \widehat{\Phi}_0' = 0 \tag{41}$$

boundary conditions are,

$$\widehat{f}_0 = \widehat{f}_0' = 0, \quad \widehat{\Phi}_0 = 1 \quad \text{at} \quad \widehat{\eta} = 0,$$
$$\widehat{f}_0' = 0, \quad \widehat{\Phi}_0 = 0 \quad \text{as} \quad \widehat{\eta} \to \infty. \tag{42}$$

For ξ^{-4},

$$\widehat{f}_1''' + \widehat{f}_1'' + n(\widehat{f}_0 \widehat{f}_0'' - \widehat{f}_0'^2) + \widehat{\Phi}_1 = 0, \tag{43}$$

$$\frac{1}{Pr} \widehat{\Phi}_1'' + \widehat{\Phi}_1' + n\left[\widehat{f}_0 \widehat{\Phi}_0' - \widehat{f}_0'(\widehat{\Phi}_0 - 1)\right] = 0 \tag{44}$$

boundary conditions are,

$$\widehat{f}_1 = \widehat{f}_1' = 0, \quad \widehat{\Phi}_1 = 1 \quad \text{at} \quad \widehat{\eta} = 0,$$
$$\widehat{f}_1' = 0, \quad \widehat{\Phi}_1 = 0 \quad \text{as} \quad \widehat{\eta} \to \infty. \tag{45}$$

The solutions of the equations (40)–(45) yields

$$\widehat{f}_0 = \frac{1}{Pr^2} + \frac{e^{-\widehat{\eta}}}{Pr(1 - Pr)} - \frac{e^{-Pr\widehat{\eta}}}{Pr^2(1 - Pr)}, \tag{46}$$

$$\widehat{f}_1 = n\left[\frac{-Pr^6 + 2Pr^4 - 7Pr^3 + 3Pr - 1}{Pr^4(1 + Pr)^2(1 - Pr)^3} - \frac{Pr^3 - Pr + 1}{Pr^3(1 - Pr)^2}\widehat{\eta}e^{-\widehat{\eta}}\right.$$
$$+ \frac{Pr^7 + Pr^6 - 3Pr^5 - 10Pr^4 + 6Pr^3 - 4Pr + 1}{Pr^4(1 + Pr)^2(1 - Pr)^3}e^{-\widehat{\eta}}$$
$$- \frac{1}{Pr^2(1 - Pr)^2}\widehat{\eta}e^{-Pr\widehat{\eta}} + \frac{-Pr^4 + 6Pr^3 - 2Pr + 1}{Pr^4(1 + Pr)(1 - Pr)^3}e^{-Pr\widehat{\eta}}$$
$$\left. - \frac{Pr^4 + Pr + 1}{Pr^4(1 + Pr)^3}e^{-(1+Pr)\widehat{\eta}}\right]. \tag{47}$$

And

$$\widehat{\Phi}_0 = e^{-Pr\widehat{\eta}}, \tag{48}$$

$$\widehat{f}_1 = n\left[\left\{\frac{1}{1+Pr} - \frac{1}{(1-Pr)^2}\right\}e^{-Pr\widehat{\eta}} + \frac{1}{1-Pr}\widehat{\eta}e^{-Pr\widehat{\eta}}\right.$$
$$\left. + \frac{1}{(1-Pr)^2}e^{-\widehat{\eta}} - \frac{1}{1+Pr}e^{-(1+Pr)\widehat{\eta}}\right]. \tag{49}$$

Finally one can find the local skin friction for large ξ as.

$$\frac{C_f}{Grx^{3/4}} = \xi^{-1}\left[\frac{1}{Pr}\right.$$
$$+ \xi^{-4}\left\{\frac{n(Pr^7+Pr^6-3Pr^5-10Pr^4+6Pr^3-4Pr+1)}{Pr^4(1+Pr)^2(1-Pr)^3}\right.$$
$$- \frac{n(Pr^4-6Pr^3+2Pr-1)}{Pr^4(1+Pr)(1-Pr)^3} - \frac{Pr^3+Pr+1}{Pr^4(1+Pr)}$$
$$\left.\left. + \frac{2Pr^3+2Pr^2-2Pr+2}{Pr^3(1-Pr)^2}\right\}\right] \tag{50}$$

when $Pr \neq 1$.

From equation (50), we can see that the skin-friction depends on suction parameter and Prandtl number Pr. But when ξ is asymptotically large (i.e. $\xi \to \infty$), the value of the skin-friction approaches to zero. We have compared the solutions obtained from the equation (50) in terms of the skin-friction with that of the other methods in Fig. 2a.

The Nusselt number is obtained as

$$\frac{Nu}{Grx^{1/4}} = \xi\left[Pr + \xi^{-4}\frac{n}{1+Pr}\right]. \tag{51}$$

From equation (51), we can see that the Nusselt number depends on the suction parameter ξ and Prandtl number Pr. We have compared the solutions obtained from the equation (51) in terms of the heat-transfer with that of the others methods in Fig. 2b.

5.3 Finite difference solution for all ξ (FD)

We have employed a most efficient solution method, known as implicit finite method, which was first introduced by Keller [21] and widely used by Hossain

et. al. [22, 23]. In this paper, the solutions are obtained for ξ and the numerical results are shown in both the tabular as well as graphical form.

To apply the aforementioned methods we first convert the equations (18) and (19) into first order system of partial differential equations.

Now the system of linear equations together with the boundary conditions can be written in matrix/vector form where the coefficient matrix has a block-tridiagonal structure. Such a system is solved using a block-matrix version of the well-known Thomas or tridiagonal matrix algorithm. The whole procedure, namely reduction to first order form followed by central difference approximations, Newton's quasi-linearisation method and the block-Thomas algorithm, is known as the Keller Box method and it was first introduced by Keller [21]. To initiate the process with $\xi = 0$, we first prescribed the guess profiles from the exact solutions of the equation (27)–(29). These profiles are then employed in the Keller-Box scheme with second order accuracy to march step by step along the boundary layer. For the given ξ the iterative procedure is stopped to give the final velocity and the temperature distribution when the difference in computing these functions in the next procedure becomes less than 10^{-5}, i.e. $|\delta f'| \leq 10^{-5}$, where the superscript denotes the number of iterations. Throughout the computations, non-uniform grids in the η direction have been incorporated, considering $\eta_j = \sinh\big((j-1)/a\big)$ where $j = 1, 2, 3, \ldots, N$ with $N = 254$ and $a = 100$, to get the quick convergence and thus save computational time and space.

6   Results and discussions

Investigation of a problem on natural convection flow from a plane vertical isothermal porous surface placed in non-isotherm surroundings has been presented here by employing three distinct solution methodologies, namely, the perturbation method for small ξ, asymptotic solution for large ξ and the Keller-box method for all values of ξ.

While $n = 1$, the ambient temperature distributions are linear. For $n < 0$, the ambient temperature decreases with x. The former of these is the more likely to occur in practical situations because this would in general represent a stable situation, i.e. a lighter fluid lies over a heavier one. For $n = 0$,

the ambient temperature remains constant. This case is very rarely achieved. When $n > 0$, the ambient temperature increases with x. This case may not occur in practical situations because this would in general represent an unstable situation, i.e. a lighter fluid lies below a heavier one.

For fluids of Prandtl number, Pr ($Pr = 0.708$ for air and $Pr = 0.10$ for mercury) takes $n = 0.3$ the numerical values of the local skin friction, $C_f/Grx^{3/4}$ and heat transfer, $Nu/Grx^{1/4}$ obtained by perturbation solution for small and large values of the transpiration parameter ξ, are depicted in Table 2 for comparison with the finite difference solution. When the Prandtl number increases the table shows that the skin friction coefficient decreases and the rate of heat transfer coefficient increases.

Fig. 2(a) and 2(b) show the influence of ambient temperature gradient n on the skin friction and local heat transfer rate. As before, the comparison shows excellent agreement between the solutions obtained by the perturbation method for small transpiration parameter and the asymptotic solutions for large transpiration parameter with the implicit finite difference solutions. From these figures we may, further, observe that an increase in the value of the parameter n leads to increase in the value of the skin-friction and decrease in value of the rate of heat transfer. Here we also observe that for each value of n there is a local maxima for skin-friction near the leading edge and then its value decreases to the asymptotic value as the value of ξ increases. The numerical values show that for $n = -0.9$, the maximum value of the local skin-friction is 084307 at $\xi = 0.54375$. The maximum value of skin-friction for $n = -0.3$ is 0.94194 which occurred at $\xi = 0.54375$. For $n = 0.0$ the maximum value is 1.00621 at $\xi = 0.58973$, for $n = 0.3$ this value is 1.06333 at $x = 0.63665$ and for $n = -0.9$ this value is 1.10552 at $\xi = 0.68459$. This implies that an increase in the value of n leads to increase in the momentum boundary layer thickness.

Now attention is given to the effect of pertinent parameters on the non-dimensional velocity and the temperature distribution in the flow field. The non-dimensional velocity and the temperature distribution are shown graphically in Fig. 3(a) and 3(b) only by the finite difference method. These figures show that the influence of the ambient temperature gradient n and the transpi-

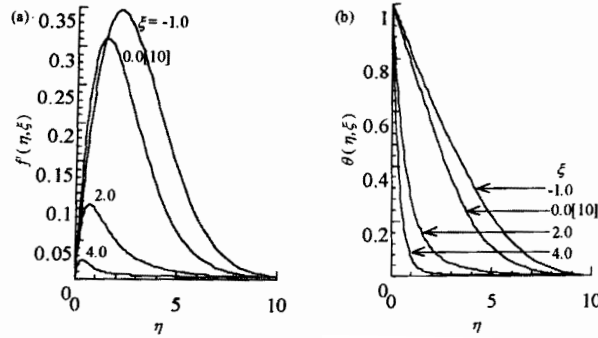ration parameter ξ on the velocity and the temperature distributions.

Fig. 3. (a) The velocity distribution and (b) the temperature distribution for different values of ξ with the selected Prandtl number $Pr = 0.708$ and $n = 0.6$.

The curves for $\xi = 0$ are found to be identical with those obtained by Cheesewright [5].

From Fig. 3 we can see that an increase in the value of the parameter n leads to increase in the velocity profile and the temperature profile and the velocity and the temperature profiles decrease with the increase of the transpiration parameter ξ. The curves for $n = 0$ are identical with those obtained by Henkes and Hoogendoorn [24]. Therefore the present results are in excellent agreement with those obtained by them. It can also be seen that at each value of the transpiration parameter ξ, there exists a local maximum value of velocity profiles in the boundary layer region. The maximum values are obtained as 0.34603, 0.31004, 0.09524, 0.02469 at $h = 2.08265$, 1.43822, 0.68459, 032549 and $x = -1.0$, 0.0, 2.0, 4.0.

Fig. 4 shows the velocity and temperature profiles for suction. When n increases the velocity and temperature increases. Fig. 5 shows a region with small backflow and temperature deficit is found in the outer part of the boundary layer in a stably stratified ($n < 0$) environment. There is no backflow or temperature deficit in an unstably stratified ($n > 0$) environment.

The comparison shows that both the skin friction and the velocity profiles are increases with the increase of the ambient temperature gradient n. The Nusselt number decreases and the temperature profile increases with the increase n, which are expected.
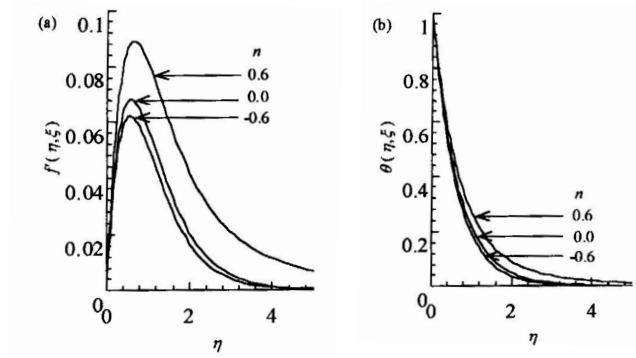
167

Fig. 4. (a) The velocity distribution and (b) the temperature distribution for different values of n with the selected Prandtl number $Pr = 0.708$, $\xi = 2.0$.
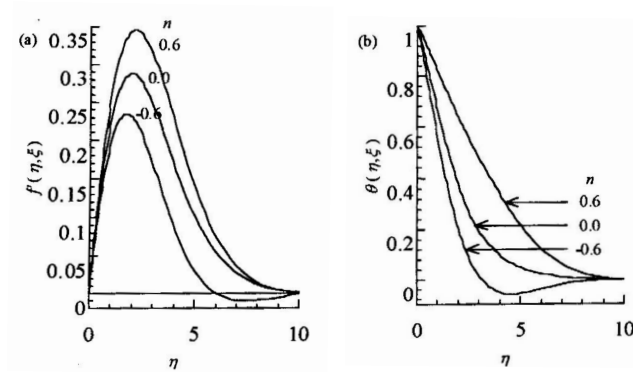

Fig. 5. (a) The velocity distribution and (b) the temperature distribution for different values of n with the selected Prandtl number $Pr = 0.708$ and $\xi = 0.6$.

References

1. Sparrow E.M., Yu H.S. "Local non-similarity thermal boundary layer solutions", *Journal of Heat Transfer,* ASME, Series C, **93**, p. 328–334, 1971

2. Kao T.T. "Laminar incompressible forced convection along a flat plate with arbitrary suction or injection at the wall", *Trans. of the ASME,* p. 484–486, 1975

3. Nachtsheim P.R., Swigert P. "Satisfaction of asymptotic boundary conditions in numerical solution of systems of non-linear equations of Boundary Layer type", *NASA TN-D* p. 3004, 1965

4. Yang K.T. "Possible similarity solutions for laminar free convection vertical plates and cylinders", *J. Appl. Mech.,* **82**, p. 230–236, 1960

5. Cheesewright R. "Natural convection from a plane vertical surface in non-isothermal surroundings", *Int. Heat Mass Transfer,* Pergamon Press Ltd. **10**, p. 1847–1859, 1967

6. Yang. K.T., Novotny J.L., Chang Y.S. "Laminar free convection from a non-isothermal plate immersed in a temperature stratified medium", *Int. Heat Mass Transfer,* **15**, p. 1097, 1972

7. Fujii T., Takeuchi M., Morioca I. "Laminar boundary layer of free convection in a temperature stratified environment", in: *Proc. 5th Int. Heat Transfer Conf. Tokeyo,* **22**, p. 44–48, 1974

8. Piau J.M. "Influence des variations des properties physiques et de la stratifica-tion en convection naturelle", *International J. Heat Mass Transfer,* **17**, p. 465–476, 1974

9. Eichhorn R., Lienhard J.H., Chen C.C. "Natural convection from isothermal spheres and cylinders immersed in a stratified fluid", in: *Proceedings, 5th International Heat Transfer Conference Tokyo,* **1.3**, p. 10–14, 1974

10. Chen C.C., Eichhorn "Natural convection from a vertical surface to a thermally stratified fluid", *ASME Journal of heat transfer,* **98**, p. 446–451, 1976

11. Venkatachala B.J., Nath G. "Non-similar laminar natural convection in a thermal stratified fluid", *Int. J. Heat Mass Transfer,* **24**(11), p. 1848–1850, 1981

12. Chamkha A.J., Khaled A.R.A. "Hydromagnetic simultaneous heat and mass transfer by mixed convection from a vertical plate embedded in a stratified porous medium with thermal dispersion effect", *Heat and Mass Transfer,* **36**, p. 63–70, 2000

13. Emmons H.W., Leigh D.C. "Tabulation Blasius function with blowing and suction", *Aero Nautical Research Council Current Papers,* C.P.N.157, 1954

14. Schlichting H., Bussemann K. "Exakte losengen fur die laminar grenzschieht mit absaugu der absblasen", *Sogruften der deutschen akert der luftfahrt-forschung, B.,* **7**(2), p. 1, 1943

15. Hartnett J.P., Eckert E.R.G. "Mass transfer cooling in a laminar boundary layer with constant fluid properties", *Trans. Amer. Soc. Mech. Engrs.,* **247**, 1957

16. Sparrow E.M., Cess R.G. *J. Heat Transfer,* **83**, p. 387, 1961

17. Merkin J.H. *Int. J. Heat Mass Transfer,* **15**, p. 989, 1972

18. Clark J.F. *J. Fluid Mech.,* **57**, p. 45, 1973

19. Aroesty J., Cole J.D. "Boundary layer flow with large injection rates", *Rand Corp Memorandum,* RM 4620 ARPA, 1965

20. Ostrach S. "An analysis of laminar natural convection flow and heat transfer about a flat plate parallel to the direction of the generating body force", NAACA TN 2635, 1952

21. Keller H.B. "Numerical method in boundary layer theory", *Annual Rev. Fluid Mech.,* 1978

22. Hossain M.A. "Viscous and Joule heating effects on MHD-free convection flow with variable plate temperature", *Int. J. Heat Mass Transfer,* **35**(12), p. 3485–3487, 1992

23. Hossain M.A., Banu N., Nakayama A. "Non-Darcy forced convection boundary layer flow over a wedge embedded in a saturated porous medium", *Numerical Heat Transfer,* **26**, Part A, p. 399–414, 1994

24. Henkes R.A.W.M., Hoogendoorn C.J. "Laminar natural convection boundary' layer flow along a heated vertical plate in a stratified environment", *Int. J. Heat Mass Transfer,* **32**, p. 147–155, 1989